Cano Embuena, AI.; Fortunati, E.; Cháfer Nácher, MT.; J.M. Kenny; Chiralt A.; González Martínez, MC. (2015). Properties and ageing behaviour of pea starch films as affected by blend with poly(Vinyl Alcohol). Food Hydrocolloids. 48:84-93. doi:10.1016/j.foodhyd.2015.01.008.

PROPERTIES AND AGEING BEHAVIOUR OF PEA STARCH FILMS AS AFFECTED BY BLEND WITH POLY(VINYL ALCOHOL).

A. Cano[a*], E. Fortunati[b], M. Cháfer[a], J.M. Kenny[b,c], A. Chiralt[a], C. González-Martínez[a]

[a]Instituto de Ingeniería de Alimentos para el Desarrollo, Universitat Politècnica de València. Camino de Vera s/n 48022 Valencia, Spain.

[b]Materials Engineering Centre, UdR INSTM, University of Perugia, Strada di Pentima 4, 05100 Terni, Italy.

[c]Institute of Polymer Science and Technology, CSIC, Juan de la Cierva 3, 28006 Madrid, Spain.

*Phone: 34-963877000 ext.83613, amcaem@upvnet.upv.es

Abstract

Pea starch (S) and poly(vinyl alcohol) (PVA) blends with different ratios were produced in order to elucidate the possible advantages of blend films to overcome the common drawbacks of starch films. Starch, poly(vinyl alcohol) and blends (S:PVA ratios of 2:1, 1:1 and 1:2) were obtained by casting and microstructure and thermal behaviour were characterized. Moreover, barrier, mechanical and optical properties were evaluated after 1 and 5 storage weeks at 25 ºC and 53 % relative humidity in order to study the effect of poly(vinyl alcohol) on the ageing process of starch. The incorporation of PVA into pea starch films implied the formation of interpenetrated networks of both incompatible polymers with partial solubilisation. S-PVA blend films were much more extensible and stable during storage, with improved water barrier properties and reduced water sorption capacity especially when the S:PVA ratio were 1:1 and 1:2. Starch-poly(vinyl alcohol) blend films are environmentally friendly, low cost materials, with good functional properties.

Keywords: Crystallization, glass transitions, mechanical properties, water vapour permeability, microstructure, polymer blends.

1. Introduction

The reduction in petroleum reserves and the great environmental impact of petroleum-derived plastics have led to the development of biodegradable materials that may be used in packaging applications. Bioplastics are biodegradable or compostable products, from renewable sources or synthesis, whose global production has increased considerably in the last few years. They have hydrolytically or enzymatically labile bonds or groups (Lu, Xiao & Xu, 2009). These biodegradable materials provide opportunities to reduce the waste through biological recycling in order to achieve a sustainable ecosystem.

Starch is considered as a bioplastic and is one of the most abundantly-occurring natural polymers, second only to cellulose (Ramaraj, 2007). It is also especially attractive because of its biodegradability and low cost (Chen, Cao, Chang & Huneault, 2008; Han, Seo, Park, Kim & Lee, 2006; Lafargue, Lourdin & Doublier, 2007). Starch has the ability to form films that are odorless, colourless, transparent, and with very low oxygen permeability (Jiménez, Fabra, Talens & Chiralt, 2012a; Vásconez, Flores, Campos, Alvarado & Gerschenson, 2009). Native starch has a granular structure and presents different properties depending on its amylose/amylopectin ratio. Gelatinized starch shows a great film-forming capacity and, as is well known, its two macromolecules are responsible for starch recrystallization, which leads to changes in the mechanical response of starch-based films (Cano, Jiménez, Cháfer, González & Chiralt, 2014; Jiménez, Fabra, Talens & Chiralt, 2012a; Talja, Helén, Roos & Jouppila, 2007). Besides their poor mechanical properties, starch films are highly hydrophilic in nature, which confers a great water vapour sensitivity and poor water barrier properties. Some authors have tried to overcome these aspects by blending starch with other compounds, such as sodium caseinate (Jiménez, Fabra, Talens & Chiralt, 2012c), sorbitan esters of fatty acids (Ortega-Toro, Jiménez, Talens & Chiralt, 2014),

63 soy protein isolate (Galus, Mathieu, Lenart, & Debeaufort, 2012; Galus, Lenart, Voilley,
64 & Debeaufort, 2013) or biodegradable synthetic polymers (Arvanitoyannis, 1999).
65 Poly(vinyl alcohol) (PVA) is a synthetic water-soluble polymer, widely used in different
66 industrial, commercial, medical and food applications (Ramaraj, 2007). PVA has been
67 extensively studied because of its biocompatibility and interesting physical properties,
68 which are due to the presence of OH groups and the hydrogen bond formation (Alexy,
69 Bakos, Hanzelova, Kukolíkova, Kupec, Charvátová, Chiellini, & Cinelli, 2003; Bonilla,
70 Fortunati, Atarés, Chiralt & Kenny, 2014). Films obtained from PVA are fully
71 biodegradable, odourless, transparent, non-toxic and have useful physical properties,
72 such as high tensile strength and flexibility, good oxygen and aroma barrier properties
73 and transparency (Ramaraj, 2007).
74 Different studies into starch-PVA blends have been carried out, focusing on
75 biodegradability studies (Gupta et al., 2014; Lu et al., 2009; Siddaramajah et al, 2004)
76 or the effect of the incorporation of different additives to the blends, such as citric acid,
77 glutaraldehyde or urea (Gupta et al 2014; Luo et al, 2012; Shi et al, 2008; Ramaraj et
78 al., 2006), calcium chloride (Jiang et al., 2012), poly(methyl methacrylate-co-
79 acrylamide) nanoparticles (Yoon et al., 2012) for different purposes (compatibility
80 enhancement or development of biomedical and packaging materials).
81 Chen et al., (2008) studied the effect of pea-starch nanocrystals (PSN) and native pea
82 starch (NPS) on the structure and physicochemical properties of the PVA films. They
83 found that PSN were more homogeneously dispersed in the PVA matrix than the NPS,
84 resulting in stronger interactions with PVA and better mechanical behaviour.
85 Sreekumar et al. (2012) found a partial miscibility of the polymers in blends of corn
86 starch and PVA, by analyzing X-ray diffraction and thermal and mechanical response.
87 Polymer compatibility and PVA crystallinity greatly decreased when the starch content
88 rose, which affected the mechanical response of the films.

Mechanical and optical properties, wide-angle X-ray scattering, and biodegradation of PVA films containing a small ratio of corn starch (0-10 %) were analyzed by Siddaramaiah et al. 2004. Although they report an increase in the haze and diffusion of light, there was only a slight change associated with the tensile behaviour of PVA films, which could be explained in terms of the changes in the crystalline structural parameters.

Pea starch is highly available and one of its advantage is its high amylose content about 24% to 65%, depending on variety (Hoover and Sosulski 1991; Han et al., 2006). In most of the cases the amylose/amylopectin ratio is higher than in corn starch. The high amylose content contributes to improve the tensile strength and gas barrier properties of starch based films (Wolff, Davis, Cluskey, Gundrum, & Rist, 1951; Lourdin, Della Valle, & Colonna, 1995; Palviainen, Heinämäki, Myllärinen, Lahtinen, Yliruusi, & Forssell, 2001; Cano et al., 2014). The very low oxygen permeability of high amylose starch films make them very useful for preservation of foods sensitive to oxidation process, such as meat and fish products or nuts. No studies have been found into the effect of PVA on the properties of gelatinized pea- starch films and on their ageing behaviour, which is one of the main drawbacks to the practical use of starch films as food packaging material. Although it could be expected a relatively close behavior of pea-starch-PVA blend films to that obtained for corn starch blends, differences in starch sources (tubercles, cereals or legumes) can imply notable changes in the film's properties (Fredriksson, Silverio, Andersson, & Eliasson, 1998; Hoover & Ratnayake, 2000). Likewise, to prove differences and similarities between starch behaviour from different sources in the films is interesting in order to their possible substitution in the industrial uses.

The aim of this work was to analyse the effect of blending different ratios of PVA and pea starch on the structure, thermal behaviour, physical properties and ageing of blend films, in order to elucidate possible beneficial effects in the starch film properties.

2. Material and Methods

2.1 Materials

Pea starch (S) was purchased from Roquette Laisa España S.A. (Benifaió, Valencia, Spain), poly(vinyl alcohol) (PVA)(M_w: 89,000-98,000, degree of hydrolysis > 99 %, and viscosity: 11.6-15.4cP) was obtained from Sigma Aldrich Química S.L. (Madrid, Spain) and glycerol and magnesium nitrate-6-hydrate were provided by Panreac Química S.A. (Castellar de Vallès, Barcelona, Spain).

2.2. Preparation of film- forming dispersions and S:PVA blend films

Films were obtained by solvent casting procedure after the preparation of film- forming dispersions (FFDs).

Starch (1% w/w) was dispersed in an aqueous solution at 95 ºC for 30 min and, while stirred, to induce starch gelatinization. Thereafter, the dispersion was homogenized using a rotor-stator homogenizer (Ultraturrax D125, Janke and Kunkel, Germany) at 13,500 rpm for 1min and 20,500 rpm for 3 min. Finally, glycerol was added at a starch:glycerol ratio of 1:0.25, on the basis of previous studies (Jiménez et al., 2012b). PVA (2% w/w) was dispersed in an aqueous solution and maintained at 90 ºC for 30 min until complete dissolution. For S-PVA blends, PVA was incorporated into the previously gelatinized starch dispersion by using S:PVA ratios of 1:2, 1:1 and 2:1 (named as S1:PVA2, S1:PVA1 and S2:PVA1, respectively). Afterwards, glycerol was also added (ratio starch:glycerol, 1:0.25).

To obtain the films, the FFDs were stirred for 30 minutes and poured into petri casting plates, in the amount which would provide a density of solid of 145 $g.m^{-2}$. Films were dried at 40 ºC in a convection oven for 48 h and afterwards, peeled off the casting surface. Films were conditioned at 53 % RH at room temperature (25±2) ºC until further analysis.

2.3. Characterization of S:PVA films

2.3.1. Fourier transform infrared spectroscopy (FT-IR)

Structural analysis was carried out by using the Fourier transform infrared spectra (FT-IR, Jasco FT-IR 615 spectrometer, Easton MD, USA). For the measurement, a few drops of solution were cast on a silicon plate for each formulation and investigated in transmission mode over the 400-4000 cm^{-1} range. Two replicates per formulation were measured.

2.3.2. Film thickness

The film thickness was measured at six random positions with a micrometer (MicrometerStarrett) to the nearest 0.001 mm.

2.3.3. Microstructure of films

The microstructural analysis of the cross-section and surface of the films was carried out using field emission scanning electron microscopy (FESEM) (Supra^{TM} 25-Zeiss, Germany). To this end, films were equilibrated at 53 % RH in desiccators by using $Mn(NO_3)_2$ solution. Two replicates per formulation were fixed on copper stubs, gold coated, and observed using an accelerating voltage of 2 and 5 kV, for the surface and cross-section observations, respectively.

2.3.4. Thermogravimetric analysis (TGA)

A thermogravimetric analyzer (Seiko Exstar 6300, Italy) was used to obtain the thermal weight loss (TG), and the derivate (DTG), of samples. To this end, the samples were heated from 30 ºC to 600 ºC at 10 ºC/min, using a nitrogen flow (250 mL/min). Prior to the analyses, the samples were conditioned at 25 ºC and 53 % RH. The thermal

degradation temperature was obtained at the maximum of the DTG curves (T_{max}). The measurements were taken in triplicate.

2.3.5. Differential scanning calorimeter (DSC)

Differential scanning calorimeter (TA Instrument, Q200, USA) measurements were carried out in triplicate under nitrogen flow in the temperature range of −25 to 250 ºC, at 10 ºC/min, by performing two heating and one cooling scan. Firstly, samples were heated from room temperature to 250 ºC at the selected heating rate and maintained for 5 min at 250 ºC. Then, samples were cooled down to -25 ºC and heated again until 250 ºC. Data were recorded during both the cooling and second heating steps. From the cooling step thermograms (heat flux vs. temperature), the crystallization temperatures (Tc) and enthalpy (ΔHc) values were obtained. Likewise, from the second heating step, the glass transition temperatures (Tg) and melting temperatures (Tm) and enthalpy values (ΔHm) were obtained. Prior to the analyses, the samples were conditioned at 25 ºC -53 % RH.

The crystallinity degree of PVA was calculated as shown in equation 1:

$$X = \frac{1}{X_{PVA}}\left[\frac{\Delta H}{\Delta H_0}\right] * 100 \quad (1)$$

Where ΔH, is the melting enthalpy of the sample, ΔH_0 , the melting enthalpy of a 100 % crystalline PVA sample (161.6 $J.g^{-1}$; Roohani, Habibi, Belgacem, Ebrahim, Karimi & Dufresne, 2008) and X_{PVA}, the mass fraction of PVA in the film.

2.3.6. Moisture content

The moisture content of the films (MC), equilibrated at 53 % RH and 25 ºC, was analysed by drying the samples in a vacuum oven at 60 ºC for 24 h. Later on, the pre-

194 dried samples were placed in desiccators containing P_2O_5 until reaching constant
195 weight. Five replicates were analysed per film formulation.
196
197 2.3.7. Water vapour permeability
198 Water vapour permeability (WVP) was evaluated in films equilibrated at 25 ºC and 53
199 % RH after 1 and 5 storage weeks, following the ASTM E96-95 gravimetric method by
200 using Payne permeability cups (Payne, elcometer SPRL, Hermelle/sd Argenteau,
201 Belgium) 3.5 cm in diameter. Deionised water was used inside the testing cup to reach
202 100% RH on one side of the film, while an oversaturated magnesium nitrate solution
203 was used to control the RH on the other side of the film. The top surface of the film
204 during drying was exposed to 100 % RH. A fan placed on the top of the cup was used
205 to reduce resistance to water vapour transport. Water vapour transmission rate
206 measurements (WVTR) were performed at 25 ºC. These conditions were chosen to
207 simulate the storage conditions of intermediate moisture foods exposed at high relative
208 humidity and at room temperature. To calculate WVTR, the slopes of the steady state
209 period of the curves of weight loss as a function of time were determined by linear
210 regression. For each type of film, WVP measurements were replicated four times and
211 WVP was calculated according to Cano et al (2014).
212
213 2.3.8. Mechanical properties
214 The mechanical properties were measured using a Universal Test Machine (Digital
215 Lloyd instrument, West Sussex, UK), following UNI ISO 527-1 (ISO, 2012), by using 5
216 cm min^{-1} and a load cell of 1.5 N. The film samples (1 x 5 cm) equilibrated at 25 ºC and
217 53 % RH (1 and 5 storage weeks) were analysed. These conditions were chosen to
218 simulate the storage conditions of intermediate moisture foods exposed at high relative
219 humidity and at room temperature. Film samples were mounted in the film-extension
220 grips (A/TG model), which were set 20 mm apart. Stress-Hencky strain curves were

obtained and the tensile strength at break (TS), percentage of elongation at break (E, %) and elastic modulus (EM) were calculated. The measurements were taken at room temperature and eight replicates carried out per formulation.

2.3.9. Ultraviolet-visible spectrophotometry

Film samples (1 x 1 cm) equilibrated at 25 ºC and 53 % RH were analysed by means of a UV–VIS spectrophotometer (Perkin Elmer Instruments, Lambda 35, Waltham, USA), by using a wavelength range between 250 and 1000 nm.

2.3.10. Internal transmittance

The transparency was determined by applying the Kubelka–Munk theory for multiple scattering to the reflection spectra obtained in a spectrocolorimeter CM-3600d (Minolta Co., Tokyo, Japan) with a 30 mm illuminated sample area. This theory assumes that each light flux which passes through the film is partially absorbed and scattered, which is quantified by the absorption (K) and the scattering (S) coefficients. Transparency (K/S) was calculated, as indicated by Hutchings (1999), from the reflectance of the sample layer on a white background of known reflectance and on an ideal black background. Measurements were taken triplicate in samples equilibrated at 25 ºC and 53 % RH for one and five weeks, using both a white and a black background.

2.3.11. Gloss

Gloss was measured using a flat surface gloss meter (Multi- Gloss 268, Minolta, Langenhagen, Germany) at an angle of 60 º with respect to the normal to the film surface, according to the ASTM standard D523 (ASTM, 1999). Prior to gloss measurements, films were conditioned at 25 ºC and 53 % RH for one and five weeks. Gloss measurements were carried out over a black matte standard plate and were

taken in triplicate. Results were expressed as gloss units, relative to a highly polished surface of standard black glass with a value close to 100.

2.4. Statistical analysis

The results were analysed by means of analysis of variance (ANOVA), using the Statgraphics Plus 5.1. Program (Manugistics Corp., Rockville, MD). Fisher's least significant difference (LSD) was used at the 95 % confidence level to distinguish the samples.

3. Results and discussion

3.1. Structure of the films

Polymer interactions in the blends lead to nano and microstructural features which are relevant in the final functional properties of the films. FTIR analyses of the samples were carried out in order to analyse particular interactions between the chains' functional groups through the shift of their specific IR bands. In this sense, hydroxyl groups of both starch and PVA chains can form hydrogen bonds, as reported by Ramaraj (2006).

Figure 1 shows FT-IR spectra for S, PVA and S:PVA blends, showing the wavenumber values corresponding to the main peaks in each sample. For every film, the broad band located between 3200-3400 cm^{-1} corresponds to the stretching vibration mode of hydroxyl groups from the absorbed water and from the polymers themselves (Chen et al., 2008; Fortunati, Puglia, Luzi, Santulli, Kenny & Torre, 2013; Jiménez, Sánchez-González, Desorby, Chiralt & Tehrany, 2013). In S and PVA films, the peak wavenumber was higher than for blend films, which showed a significant peak shift (about 40 cm^{-1}), in agreement with the promotion of hydrogen bond formation between the hydroxyl groups of both polymers. The peak associated with the bending vibration mode of hydroxyl group appears between 1400-1460 cm^{-1} and was slightly displaced

274 for S and PVA (1455 and 1420 cm^{-1}, respectively). In blend films, this peak was also
275 shifted towards a lower wavenumber in agreement with the formation of hydrogen
276 bonds, as mentioned above. The peak located between 2910-2935 cm^{-1} is related with
277 C-H stretching (Fortunati et al., 2013; Jagadish & Raj., 2011; Jiménez et al., 2013) and
278 appeared with different intensities for S and PVA films. In the blends, this peak was
279 shifted to a higher wavenumber. The peak at 1731 cm^{-1} has been assigned to the C-C-
280 O stretching in starch films (Jagadish & Raj., 2011). In PVA and blend films, this peak
281 greatly decreased in intensity despite the high ratio of starch in the S2:PVA1 film.
282 Moreover, this peak shifts to a lower wavenumber in blend films. The stretching
283 vibration of C-O in C-C-O and in the glucose ring in starch corresponds to the peaks at
284 1024 and 860 cm^{-1}, respectively, and also appeared with lesser intensity and a slight
285 shift in the blend films. For PVA films, C-O stretching vibration appeared at 1094 cm^{-1},
286 according to Chen et al., 2008. These results highlight the formation of hydrogen bonds
287 to some extent between the hydroxyl groups of the starch polymers and PVA chains,
288 and point to a certain degree of polymer miscibility.
289 Figures 2 and 3 show the FESEM images of the surface and cross section of the
290 different films. S films had a smooth surface and a homogeneous internal structure,
291 typical of gelatinized starch, as was found in other studies (Cano et al., 2014; Chen,
292 Liu, Chang, Cao & Anderson, 2009; Wu, Liu, Chen, Chen, Anderson, & Chang, 2010).
293 Nevertheless, the presence of a heterogeneously-fractured layer near the film surface
294 reveals the progress of crystallization in this zone, probably due to the greater
295 molecular mobility associated with the diffusion of water vapour to the film surface
296 (Cano et al., 2014).
297 PVA films also exhibited a smooth surface. Nevertheless, the cross section images
298 revealed the presence of zones with different morphology which could be attributed to
299 the coexistence of amorphous and crystalline regions in the film. The chain
300 associations in crystalline regions will define a different morphology from that of the

amorphous zones, coinciding with that reported by other authors (Bonilla et al., 2013; Chen et al., 2008; Fortunati et al., 2013). Blend films (Figure 2) showed rougher, irregular surfaces, especially when the proportion of PVA in the blend was equal or higher than that of the starch. This indicates polymer incompatibility and the formation of two phases: one PVA-rich phase and another starch-rich phase, which emerge to the surface in a differentiated way when starch is present at equal or lower ratio than PVA. For the highest starch ratio, this polymer forms a more continuous phase and no particles were observed at the film surface. The cross section images of blend films also exhibit this phase separation, which gives rise to two interpenetrated networks of both polymers where the zones with different morphology for PVA can also be appreciated. The phase separation of both polymers in corn starch and PVA blend films has also been reported by Sreekumar et al (2012).

3.2. Thermal behaviour

The thermal behaviour of the films was analysed by TGA and DSC measurements, in order to find out the thermal stability of polymers (Adbelrazek et al., 2010) and to highlight the effect of the different S:PVA ratios on the thermal degradation pattern, as well as the phase transitions in the films in the processing/handling temperature range.

Figure 4 shows the weight loss (TG) and derivate (DTG) curves for S, PVA and S:PVA blend films obtained by thermogravimetric analysis while the temperatures for the main degradation step of the films are summarized in Table 1. For pure starch films, two weight loss steps were observed. The initial weight loss (first peak),up to about 100 ºC, can be attributed to the loss of bonded water in the film (Luo, Li & Lina, 2012). In the second step, between 170-450 ºC, about 70 % of the sample weight was lost, which is related to the main degradation process (peak temperature: 315 ºC). For PVA films, three weight loss steps were observed in Figure 4. As in the S films, the initial step, up to about 100 ºC, can be attributed to the loss of adsorbed and bound water (Bonilla et

al., 2013). The second step occurs between 200-400 ºC, in which the dehydration of the PVA takes place, followed by chain scission and decomposition (Frone, Panaitescu, Donescu, Spataru, Radovic & Trusca, 2011; Li, Yue, & Liu, 2012). The third step occurs between 400 – 500 ºC and it can be attributed to the degradation of the by-products generated by PVA during the thermal process (Bonilla et al., 2013; Lewandowska, 2009). Similar three-step weight loss behaviour was observed for the S:PVA blends, except for the film with the lowest PVA ratio (S2:PVA1), where a second weight loss step was observed after the first water loss, at relatively low temperature (150-200 ºC). This could indicate either that PVA starts to degrade at very low temperatures when it is present in the blend at the lowest ratio, or that the PVA hydroxyl groups react with those of starch chains through the formation of oxi (-O-) groups with subsequent water loss. Sreekumar et al. (2012) also observed similar behaviour when analysing corn starch PVA blend films obtained by casting.

Mean values exhibit significant differences ($p<0.05$) for the different formulations, indicating that PVA films degrade at the lowest temperature (279 ºC), although S:PVA blends with the highest PVA ratio showed slightly greater thermal stability, with higher values of the degradation temperature, similar to that of the starch (Table 1). The blend with the lowest ratio of PVA exhibited anomalous thermal behaviour, showing the first small degradation peak at 172 ºC.

Tables 1 and 2 show the results obtained from the DSC analysis, in terms of glass transition (Tg), crystallization (Tc) and melting temperatures (Tm), enthalpy of crystallization (ΔHc) and melting (ΔHm) and percentage of crystallinity (X) of PVA.

The cooling scan of the samples showed different peaks associated with the crystallization of PVA. Starch films do not show crystallization peaks or crystallite melting. The crystallization temperature (Tc) values for the different crystallization peaks of PVA are shown in table 1. Two peaks at 140 (secondary peak) and 201 ºC (main peak) were observed for PVA films, which could be due to the fact that the

crystallization of some molecules is delayed by steric hindrances at the end of the crystallization process. This usually occurred in complex mixtures, when the molecular mobility of the polymer chain segments was limited. Likewise, some trends were observed in the crystallization behaviour of PVA, due to the incorporation of starch. As in PVA, two crystallization peaks were observed for the blend films with the highest PVA ratio, but at a higher temperature for the secondary peak (178 ºC). For the greatest PVA ratio in the blend, three crystallization peaks were observed. The greater the starch ratio in the blend, the higher the Tc values of the main peak (at 209 ºC), with two secondary peaks at 200 and 178 ºC. These results suggest that starch enhanced the crystallization rate of PVA, since less undercooling was required.

The melting temperature of PVA is 227 ºC, without the split observed in crystallization. This value coincides with those reported by other authors (Bonilla et al., 2013; Mailo, Gonzalez, Hoppe & Alvarez, 2011). No differences in the Tm of PVA were observed for blend films with the lowest PVA ratio. However, in the other blends with a higher ratio of PVA, two melting peaks were observed at 226 and at about 210 ºC. This suggests that PVA polymorphism was promoted when a high proportion of starch was present in the film, thus showing two melting intervals. The differences between crystallization and melting behaviour are explained in terms of kinetic hindrances which take place during the crystallization process. In this sense, notable differences can be found between the obtained Tc and Tm temperatures; the latter is the equilibrium value and the former is affected by crystallization kinetics.

The crystallization and melting enthalpies of PVA in the different films are shown in Table 2, expressed as $J.g^{-1}$ of sample and $J.g^{-1}$ of PVA in the film, and deduced from the additive integration of all the melting peaks in the thermogram. As expected, the greater the PVA content in the film, the higher the enthalpy value. No significant differences were observed between the ΔHm and ΔHc values, which indicates that no undercooling occurred during the cooling step. The crystallinity of PVA was obtained

382 from the ΔHm values (J.g^{-1} PVA), taking the ΔHm reported (Roohani et al., 2008) for
383 100 % crystallized PVA (161.6 J.g^{-1} PVA) into account. The crystallinity values are
384 shown in Table 2, where the inhibition of PVA crystallization brought about by the
385 starch blend can be observed for films containing the same ratio of starch and PVA. An
386 increased variability in the values can also be observed in blend films, which can be
387 attributed to a kinetic control of the polymer chain interactions during crystallization.
388 Taking the variability into account, it is remarkable that no significant inhibition of PVA
389 crystallization occurs in the other blend films with different ratios of PVA and S.
390 As far as glass transition is concerned, starch films showed the highest Tg value (160
391 ºC), which was similar to that reported by other authors for starch films (Ortega-Toro,
392 Jiménez, Talens, & Chiralt, 2014b), while the PVA amorphous phase showed lower Tg
393 values (79 ºC) in agreement with that previously reported (Fortunati et al., 2013). Two
394 glass transitions were observed in thermograms of blend films, one for each polymer
395 phase, in agreement with the phase separation of the polymers commented on above.
396 The Tg of the PVA rich phase did not significantly change with respect to the pure PVA,
397 except for the S1:PVA1 blend, where an increase in the Tg value can be observed.
398 This indicates that starch (with a higher molecular weight) partially solubilises in the
399 PVA phase, thus promoting an increase in the Tg in the blend with the same ratio of
400 polymers. On the contrary, the Tg values of the starch rich phase decreased when the
401 PVA (lower molecular weight) was solubilised in this phase, and this effect was more
402 intense at the highest ratio of starch in the film. So, the partial compatibility of the
403 polymer was dependent on the polymer ratio, as reported by Sreekumar et al. 2012;
404 the highest degree of starch miscibility in PVA films occurred at the ratio of 1:1, while
405 the PVA solubilizes in the starch phase at all the tested starch ratios.
406 An analysis of the thermal behaviour of S:PVA blends, as compared with non-blend
407 polymers, indicates that both polymers show partial miscibility, which depended on the
408 polymer ratio, and which affected the behaviour of PVA crystallization and the glass

409 transition of the different phases in the films. In blends with the S1:PVA1 ratio, PVA
410 crystallization was significantly inhibited while the Tg of amorphous PVA significantly
411 increased with respect to pure PVA. This indicates that, at this ratio, interactions of
412 starch molecules in the PVA phase were enhanced, and the blend effects were
413 intense. However, the starch rich phase is affected by PVA molecules (lower Tg),
414 especially at the highest S ratio.
415
416 3.3. Water vapour barrier properties of the films
417 Table 3 shows the water vapour permeability values (WVP) of the films at 25 ºC and a
418 53-100 % RH gradient, together with their equilibrium moisture content and thickness.
419 The moisture content of the films ranged between 5 and 8 %, the S films exhibiting
420 higher values ($p<0.05$) than the PVA films, coherent with their more hydrophilic nature
421 (a higher ratio of hydroxyl groups). PVA is water-soluble and starch is water-sensitive,
422 which leads to their blends being water sensitive (Chen et al., 2008). S:PVA blends had
423 moisture contents that were more similar to S than to PVA films, showing significant
424 differences ($p<0.05$) with respect to the latter. The higher the starch contents in the
425 films, the greater their equilibrium moisture content. The moisture content of the
426 samples tends to increase throughout 5 storage weeks, but only S and PVA films
427 showed significant differences ($p<0.05$) after the storage time. This fact indicate that
428 films equilibrate slowly with the conditioning relative humidity, approaching equilibrium
429 value after 5 weeks' storage.
430 The WVP values define the final application of a film in contact with food systems and
431 they must be as low as possible so as to avoid water transfer (Ma, Chang & Yu, 2008).
432 Significant differences between the WVP values of the different films are found after
433 the two different storage times, which coincides with results found by other authors
434 studying pea starch films (Cano et al., 2014; Han et al., 2006; Ma et al., 2008) and PVA
435 films (Bonilla et al., 2013). Pea starch films showed the highest WVP (5.03 g.mm.kPa^{-}

436 $^{1}.h^{-1}.m\text{-}^{2}$), while PVA films were less permeable (2.2 $g.mm.kPa^{-1}.h^{-1}.m^{-2}$) and S:PVA
437 blends had intermediate WVP values. The higher the starch content, the more
438 permeable the films are to water vapour. After five storage weeks, the WVP only
439 significantly changed for S films, a fact which could be related with the increase in
440 moisture content and the structural changes which occurred in the starch matrix.
441 Several authors reported that starch microstructure changes throughout storage time in
442 line with the progress of the recrystallization process or chain aggregation, thus giving
443 rise to changes in barrier and mechanical properties (Cano et al., 2014; Jiménez et al.
444 2012b). In this sense, PVA incorporation into the starch matrix seems to limit structural
445 changes, as deduced from the stability of water vapour permeability values.
446 The differences in the WVP values of S and PVA films are related with the different
447 hydrophilic nature of the polymers. In both, hydroxyl groups favour water affinity but
448 their distribution and density in the chains establish relevant differences in the water
449 sorption capacity and the mass transfer rate of water molecules. As previously
450 commented, RH gradient used was chosen to simulate the storage conditions of
451 intermediate moisture foods exposed at high relative humidity and at room
452 temperature. In this sense, it is remarkable that, due to the water sensitivity of polymer
453 blend, at lower RH conditions better water vapour barrier of the films can be expected,
454 in line with the reduced mean water content of the film and the subsequent diminution
455 of molecular mobility and diffusion properties.
456 The different polymer and water interactions also affected the film thickness. Table 3
457 shows these values, where the lower thickness values for starch films than for PVA
458 films can be observed. This indicates that a best chain packaging occurs in starch
459 matrix, whereas PVA chains are less densely packed. For blend films, intermediate
460 thickness values were obtained, regardless of the polymer ratio. No significant changes
461 ($p>0.05$) in film thickness were observed throughout storage time, despite the increase
462 in moisture content in some cases. The small differences in the film thickness could

affect the obtained values of barrier and mechanical properties of the films, although this parameter is included in the models used to determine these properties. In fact Yeun et al., 2005 found that oxygen permeability tend to decreased when the film thickness increased in PVA hybrid films.

3.4. Mechanical properties

Figure 5 shows the typical stress-strain curves obtained for all the films after one and five storage weeks under controlled conditions (53 % RH and 25 ºC), where the different mechanical behaviour of the matrices and the effect of ageing can be observed. Although starch films exhibited the typical mechanical behaviour of a brittle material, without plastic deformation and with very low extensibility at break, the great resistance to break of PVA is highlighted.

Elastic modulus (EM), tensile strength at break (TS) and percentage of elongation at break (E, %) are the parameters used to describe the mechanical behaviour of films. Table 4 shows the mean values of these parameters for the S films, PVA films and S:PVA blend films. The obtained values are coherent with those reported by other authors working on pea starch films (Cano et al., 2014; Da Matta, Silveira, de Oliveira & Sandoval, 2011), PVA films (Chen et al., 2008; Fortunati et al., 2013) and S:PVA blend films (Shi, Bi, Zhang, Zhu, Chen, Zhou, Zhang & Tian, 2008; Yoon, Park & Byun, 2012). The S films were stiffer than the PVA films, but the latter showed highest break strength and stretchability values.

In the case of the S films, every parameter significantly changes during storage. The films become harder, more resistant to break, but more brittle and less stretchable, as previously reported by Cano et al. (2014). The stiffness of the PVA films also slightly increased, but their resistance to break and extensibility did not change, the latter being much higher for PVA than for the S films. The blend films were the least stiff, with no significant differences between blends; the elastic modulus slightly increased during

storage, especially when the S ratio was the greatest. These films also exhibited the lowest resistance to break, while maintaining high values of stretchability. Both resistance and extensibility decreased when the S ratio increased in the blend.

The effect of storage time on these parameters was only appreciated at the highest S ratio where the films underwent a significant loss in extensibility. The changes in mechanical behaviour during storage are related with the structural changes in the film associated with the progressive formation of hydrogen bonds, reinforcing the interchain forces (Myllärinen, Buleon, Lahtinen & Forssell, 2002; Rindlav, Hulleman, & Gatenholm, 1997). This increase in the interchain forces could be related with a potential glycerol migration throughout the storage time, which would lead to the establishment of the hydrogen bonds between chains, thus increasing the film toughness and reducing their extensibility. However, these effects were observed in all samples, included the neat PVA films which do not contain glycerol. So, the progressive chain aggregation throughout storage time occurred in all cases, thus affecting mechanical behaviour. Nevertheless, the incorporation of PVA into starch films seems to limit these changes, giving rise to more stable films from the mechanical point of view, while conferring better flexibility and extensibility to the blend films, with high values of hardness and mechanical resistance.

The mechanical behaviour of blend films is coherent with the formation of two interpenetrated networks of both polymer phases with partial chain miscibility, as deduced from the microstructural and phase transition analyses.

3.5. Optical properties

The optical properties, UV-VIS spectra, transparency (Ti) and gloss of the films are also directly related with their microstructure, respectively and are affected by the surface and internal heterogeneity of the structure (Jiménez et al., 2012a).

516 The UV-VIS spectra of the pea starch, PVA and S:PVA blend films are shown in Figure
517 6. The S, PVA and the blend with the ratio of 1:2 S:PVA exhibit higher values of
518 transmittance (T) in the visible light range (400-800 nm) than in the UV range (200-400
519 nm), according to what is reported by Chen et al., (2008) for PVA films. In the range of
520 visible light, the T values are over 90 %, indicating a good transparency. The blend
521 films with S:PVA ratios of 1:1 and 2:1 showed the highest values of T, while the S and
522 PVA films and 1:2 blend films exhibited lower T values, especially in the UV range.
523 Therefore, in terms of light transmission no additive behaviour of the polymer contents
524 in the blends can be inferred from visible spectra. In the UV range, differences between
525 the spectra grew and the blends with S:PVA ratios of 1:1 and 2:1 had the highest
526 transmittance values. These results confirm the interactions between the PVA and S
527 chains that greatly modify the UV-light interactions of the blends, as compared with the
528 PVA or S films. 1:1 and 2:1 S:PVA blends were more transparent to UV radiation,
529 which represents a drawback in terms of the protection of food against oxidative
530 processes or other UV induced reactions.
531 In terms of internal transmittance at 450 (Ti) nm (Table 5), all the films showed a similar
532 degree of transparency which did not significantly change during storage time and the
533 differences in the film structure did not notably affect the film appearance. As for the
534 film gloss, the PVA films are the glossiest, while the blend films exhibit the lowest gloss
535 values due to the appearance of surface roughness associated with the presence of
536 the two polymer phases, as commented on above. In general, except for the S films,
537 the gloss values were quite stable during storage (Table 5). A reduction of the gloss in
538 starch films during storage was previously reported and attributed to crystalline
539 formation at surface level, where water sorption occurs, inducing molecular mobility
540 (Cano, et al. 2014; Jiménez et al 2012b).
541

542 **4. Conclusions**

543 The incorporation of PVA into pea starch blends implied the formation of
544 interpenetrated networks of both incompatible polymers with the partial solubilisation of
545 each one in the other polymer phase, depending on the polymer ratio. This has
546 beneficial effects on the mechanical properties of the films, these becoming much more
547 extensible and stable during storage. The water barrier properties were also improved
548 by PVA blending at a S:PVA ratio of under 50%, when films also reduced their water
549 content as compared to the S films. The blends did not lead to a notable loss of
550 transparency or gloss as compared to starch films and maintained their optical
551 characteristics during storage, which did not occur in pure starch films. So,
552 incorporating PVA to the S films at a ratio of around 1:1 represents a good strategy for
553 improving the functionality of starch films without a notable increase in cost.
554
555 **Acknowledgments**
556 The authors acknowledge the financial support from the Spanish Ministerio de
557 Economía y Competitividad throughout the project AGL2010-20694, co-financed with
558 FEDER funds. Amalia Cano also thanks the Spanish Ministerio de Educación, Cultura
559 y Deporte for the FPU grant and COST-STSM-FA1001-14253 for the financial support
560 for the collaboration.
561
562 **REFERENCES**
563 – Abdelrazek, E. M., Elashmawi, I. S., & Labeeb, S. (2010). Chitosan filler effects on
564 the experimental characterization, spectroscopic investigation and thermal studies of
565 PVA/PVP blend films. Physica B, 405, 2021-2027.
566 – Alexy, P., Bakos, D., Hanzelova, S., Kukolíkova, L., Kupec, J., Charvátová, K.,
567 Chiellini, E. & Cinelli, P. (2003). Poly(vinyl alcohol)-collagen hydrolysate
568 thermoplastic blends: I. Experimental design optimisation and biodegradation
569 behaviour. *Polymer Testing,* 22, 801-809.

570 – Arvanitoyannins I.S. 1999. Totally and partially biodegradable polymer blends based
571 on natural and synthetic macromolecules: preparation, physical properties and
572 potential as food packaging materials. *Journal of Macromolecular Science-Reviews*
573 *in Macromolecular Chemestry & Physics*, 39, 205-271.
574 – ASTM. (1995). Standard test methods for water vapour transmission of materials.
575 Standard designations: E96-95 Annual book of ASTM standards. Philadelphia, PA:
576 American Society for Testing and Materials. (pp. 406 e 413).
577 – ASTM. (1999). Standard test methods for specular gloss. Designation (D523). In
578 Annual book of ASTM standards, Vol. 06.01. Philadelphia, PA: American Society for
579 Testing and Materials.
580 – Bonilla, J., Fortunati, E., Atarés, L., Chiral, A., & Kenny, J.M. (2014). Physical,
581 structural and antimicrobial properties of poly vinyl alcohol-chitosan biodegradable
582 films. *Food Hydrocolloids*, 35, 463-470.
583 – Cano, A., Jiménez, A., Cháfer, M., González, C., & Chiralt, A. (2014). Effect of
584 amylose:amylopectin ratio and rice bran addition on starch films properties.
585 *Carbohydrate Polymers*, 111, 543-555.
586 – Chen, J., Liu, Ch., Chen, Y., Chen Y., & Chang, P.R. (2008). Comparative study on
587 the films of poly(vinyl alcohol)/pea starch nanocrystals and poly(vinyl alcohol)/native
588 pea starch. *Carbohydrate Polymers*, 73, 8-17.
589 – Chen, Y., Liu, Ch., Chang, P.R., Cao, X., & Anderson, D.P. (2009).
590 Bionanocomposites based on pea starch and cellulose nanowhiskers hydrolyzed
591 from pea hull fibre: Effect of hydrolysis time. *Carbohydrate Polymers*, 76, 607-615.
592 – Da Matta, M.D., Silveira, S.B., de Oliveira, L.M., & Sandoval, S. (2011). Mechanical
593 properties of pea starch films associated with xanthan gum and glycerol. *Starch*, 63,
594 274-282.

595 – Fortunati, E., Puglia, D., Luzi, F., Santulli, C., Kenny, J.M., & Torre, L. (2013). Binary
596 PVA bio-nanocomposites containing cellulose nanocrystals extracted from different
597 natural sources: Part I. *Carbohydrates Polymers,* 97, 825-836.
598 – Fredriksson, H., Silverio, J., Andersson, R., & Eliasson, P. (1998). The influence of
599 amylose and amylopectin characteristics on gelatinization and retrogradation
600 properties of different starch. *Carbohydrate Polymers*, 35, 119-134.
601 – Frone, A. N., Panaitescu, D. M., Donescu, D., Spataru, C. I., Radovici, C., & Trusca,
602 R., (2011). Preparation and characterization of PVA composites with cellulose
603 nanofibers obtained by ultrasonication. *BioResources*, 6, 487–512.
604 – Galus S., Mathieu H., Lenart A., & Debeaufort F. (2012). Effect of modified starch or
605 maltodextrines incorporation on the barrier and mechanical properties, moisture
606 sensitivity and appearance of soy protein isolate-based edible films. *Innovative Food*
607 *Science and Emerging Technologies*,16, 148-154.
608 – Galus S., Lenart A., Voilley A., & Debeaufort F. (2013). Effect of oxidized potato
609 starch on the physicochemical properties of soy protein isolate-based edible films.
610 *Food Technology and Biotechnology*, 5 (3), 403-409.
611 – Han, J.H., Seo, G.H., Park, I.I., Kim, G.N., & Lee, D.S. (2006). Physical and
612 mechanical properties of pea starch edible films containing beeswax emulsions.
613 *Food engineering and physical properties*, 71 (6), 290-296.
614 – Hoover, R., & Sosulski, F.W. (1991).Composition, structure, functionality and
615 chemical modification of legume starches*. Canadian Journal Physiology and*
616 *Pharmacology, 69, 79–92.*
617 – Hoover, R., & Ratnayake, W.S. (2002). Starch characteristics of black bean, chick
618 pea, lentil, navy bean and pinto bean cultivars grown in Canada. *Food Chemestry*,
619 78(4), 489-498.
620 – Hutchings, J.B. (1999). Food and Colour Appearance, Second Edition.
621 Gaithersburg, Maryland: Chapman and Hall Food Science Book, Aspen Publication.

622 – Jagadish, R.S., & Raj, B. (2011). Properties and sorption studies of polyethylene
623 oxide-starch blended films. *Food Hydrocolloids,* 25, 1572-1580.
624 – Jiménez, A., Fabra, M.J., Talens, P., & Chiralt, A. (2012a). Edible and
625 biodegradable starch films: A review. *Food Bioprocess Technol*, 5(6), 2058-2076.
626 – Jiménez, A., Fabra, M.J., Talens, P., & Chiralt, A. (2012b). Effect of re-crystallization
627 on tensile, optical and water vapour barrier properties of corn starch films containing
628 fatty acids. *Food Hydrocolloids*, 26, 302-310.
629 – Jiménez, A., Fabra, M.J., Talens, P., & Chiralt, A. (2012c). Effect of sodium
630 caseinate on properties and ageing behaviour of corn starch based films. *Food*
631 *Hydrocolloids*, 29 (2), 265-271.
632 – Jiménez, A., Sánchez-González, L., Desorby, S., Chiralt, A. & Tehrany, E.A. (2013).
633 Influence of nanoliposomes incorporation on properties of film forming dispersions
634 and films based on corn starch and sodium caseinate. *Food Hydrocolloids,* 35, 159-
635 169.
636 – ISO 527-1. (2012). Plastics and determination of tensile properties. Part 1: General
637 principles.
638 – Lafargue, D., Lourdin, D., & Doublier, J.L. (2007). Film-forming properties of a
639 modified starch/k-carrageenan mixture in relation to its rheological behavior.
640 *Carbohydrate Polymers*, 70, 101-111.
641 – Lewandowska, K. (2009). Miscibility and thermal stability of poly(vinyl alcohol)/
642 chitosan mixtures. *Thermochimica Acta*, 493, 42-48.
643 – Lourdin, D., Della Valle, G., Colonna, P. (1995). Influence of amylose content on
644 starch films and foams. *Carbohydrate Polymers*, 27, 261–70.
645 – Li, W., Yue, J., & Liu, S. (2012). Preparation of nanocrystalline cellulose via
646 ultrasound and its reinforcement capability for poly(vinil alcohol) composites.
647 *Ultrasonics Sonochemistry*, 19, 479–485.

- Lu, D.R., Xiao, C.M. & Xu, S.J., (2009). Starch-based completely biodegradable polymer materials. –*eXPRESS Polymer Letters*, 3, 366-375.
- Luo, X., Li, J. & Lin, X. (2012). Effect of gelatinization and additives on morphology and thermal behavior of cornstarch/PVA blend films. *Carbohydrates Polymers*, 90, 1595-1600.
- Ma, X., Chang, P.R., & Yu, J. (2008). Properties of biodegradable thermoplastic pea starch/carboxymethyl cellulose and pea starch/microcrystalline cellulose composites. *Carbohydrate Polymers*, 72, 369-375.
- Mailo, S.A., Gonzalez, J.S., Hoppe, C & Alvarez, V.A. (2011). Geles compuestos basados en poli(vinil alcohol) para su uso en biomedicina. 11º Congreso Binacional de Metalurgia y Materiales SAM / CONAMET 2011.
- Myllärinen, P., Buleon, A., Lahtinen, R., & Forssell, P. (2002). The crystallinity of amylose and amylopectin films. *Carbohydrate Polymers,* 48, 41-48.
- Ortega, R., Jiménez, A., Talens, P., & Chiralt, A., (2014b). Properties of starch–hydroxypropyl methylcellulose based films obtained by compression molding. *Carbohydrate Polymers,* 109, 155–165.
- Ortega-Toro, R., Jiménez, A., Talens, P & Chiralt, A. (2014a). Effect of the incorporation of surfactants on the physical properties of corn starch films. *Food Hydrocolloids,* 38, 66-75.
- Palviainen, P., Heinämäki, J., Myllärinen, P., Lahtinen, R., Yliruusi, J., & Forssell, P. 2001. Corn starches as film formers in aqueous-based film coating. *Pharmaceutical, Development and Technology*, 6,353–61.
- Ramaraj, B. (2007). Crosslinked poly(vinyl alcohol) and starch composite films. II. Physicomechanical, thermal properties and swelling studies. *Journal of Applied Polymer Science,* 103, 909-916.

673 – Ramaraj, B. (2006). Mechanical, thermal and morphological properties of
674 environmentally degradable ABS and poly(vinyl alcohol) blends. *Journal of Applied*
675 *Polymer Science,* 106, 1048-1052.
676 – Rindlav,A., Hulleman, S.H.D., & Gatenholm, P. (1997). Formation of starch films
677 with varying crystallinity. *Carbohydrate Polymers,* 34, 25-30.
678 – Roohani, M., Habibi, Y., Belgacem, N.M., Ebrahim, G., NaghiKarimi, A., & Dufresne,
679 A. (2008). Cellulose whiskers reinforced polyvinyl alcohol copolymers
680 Nanocomposites. *European Polymer Journal*, 44, 2489–2498.
681 – Roy, S., Gennadios, A., Weller, C.L., Testin, R.F. (2000). Water vapor transport
682 parameters of a cast wheat gluten film. *Industrial Crops and Products*. 11, 43–50.
683 – Shi, R., Bi, J., Zhang, Z., Zhu, A., Chen, D., Zhou, X., Zhang, L., Tian, W. (2008).
684 The effect of citric acid on the structural properties and cytotoxicity of the
685 polyvinylalcohol/starch films when molding at high temperature. *Carbohydrate*
686 *Polymers*, 74, 763–770.
687 – Siddaramaiah, Raj, B., & Somashekar, R. (2004). Structure–property relation in
688 polyvinyl alcohol/starch composites. *Journal of Applied Polymer Science*, 9, 630–
689 635.
690 - Sreekumar, P.A., Al-Harthi,M.A., & De, S.K. (2012). Studies on compatibility of
691 biodegradable starch/polyvinyl alcohol blends. *Polymer engineering and science*,
692 52(10), 2167-2172.
693 - Talja, R. A., Helén, H., Roos, Y. H., & Jouppila, K. (2007). Effect of various polyols
694 and polyol contents on physical and mechanical properties of potato starch-based
695 films. *Carbohydrate Polymers*, 67(3), 288-295.
696 - Vásconez, M.B., Flores, S.K., Campos, C.A., Alvarado, J., & Gerschenson, L.N.
697 (2009). Antimicrobial activity and physical properties of chitosan-tapioca starch
698 based edible films and coatings. *Food Research International*, 42, 762-769.

- Wolff, I.A., Davis, H.A., Cluskey, J.E., Gundrum, L.J., & Rist, C.E. (1951). Preparation of films from amylose. *Industrial & Engineering Chemestry Research*, 43, 915–9.
- Wu, H., Liu, Ch., Chen, J., Chen, Y., Anderson, D.P., & Chang, P.R. (2010). Oxidized pea starch/chitosan composite films: Structural characterization and properties. *Journal of Applied Polymer Science*, 118, 3082-3088.
- Yoon, S., Park, M. & Byun, H. (2012). Mechanical and water barrier properties of starch/PVA composite films by adding nano-sized poly(methylmethacrylate-co-acrylamide) particles. *Carbohydrate Polymers,* 87, 676– 686.
- Zhang, W., Yang, X., Li, C., Liang, M., Lu, C. & Deng, Y. (2011). Mechanical activation of cellulose and its thermoplastic polyvinyl alcohol composites with enhanced physicochemical properties. *Carbohydrate Polymers*, 83, 257-263.

711 **Table 1.** Crystallization, glass transition and melting temperatures of S, PVA and S:PVA blend films obtained by DSC and the degradation

712 temperatures (Tmax) obtained from TGA analysis.

713

	Cooling scan			Second heating scan				
	Tc_1 (ºC)	Tc_2 (ºC)	Tc_3 (ºC)	Tm_1 (ºC)	Tm_2 (ºC)	Tg_1 (ºC)	Tg_2 (ºC)	Tmax (ºC) *
S							160±3[a]	315±2[a]
PVA	140.7±1.7[a]	201.52±0.06[a]			227.3±0.4[a]	79.3±0.2[a]		279±3[b]
S1:PVA2	178.4±1.2[bc]	196.9±1.3[b]			226.4±1.3[a]	76±4[a]	124±2[a]	374.3±0.4[c]
S1:PVA1	179±3[b]	200±2[ab]	209.1±0.2[b]	212.2±1.9[a]	226.2±1.4[a]	89±11[b]	124±10[a]	307±5[d]
S2:PVA1	175±2[c]	199.8±0.7[a]	209.2±0.2[b]	207±4[a]	226.43±0.06[a]	78±3[a]	113.1±0.8[b]	304.6±1.6[d]

714 (*) A previous peak with smaller weight loss at 172.09±0.54 ºC was observed.

715 Tg: glass transition temperature; Tc: crystallization temperature; Tm: melting temperature and Tmax: temperature at maximum decomposition rate.

716 [a,b,c,d] different letters in the same column indicate significant differences among formulations ($p<0.05$).

717 **Table 2.** The crystallization and melting enthalpy of S, PVA and S:PVA blend films

718 obtained by DSC.

719

	Cooling scan		Second heating scan		
	ΔHc (J g^{-1})	ΔHc (J g^{-1}PVA)	ΔHm (J g^{-1})	ΔHm (J g^{-1}PVA)	X (%)
S					
PVA	72±2[a]	77±2[ab]	73.8±0.2[a]	78.6±0.3[ab]	49.7±0.3[a]
S1:PVA2	30±3[b]	49±4[c]	49±7[b]	79±11[b]	49±7[a]
S1:PVA1	31±8[b]	69±19[c]	21±1[c]	47±2[c]	29.2±1.4[b]
S2:PVA1	27±5[a]	87±16[b]	18±5[c]	61±19[c]	43±4[a]

720 ΔHc: enthalpy of crystallization; ΔHm: enthalpy of fusion and X: crystallinity.

721 [a,b,c] different letters in the same column indicate significant differences among formulations ($p<0.05$).

722

723 **Table 3.** Moisture content (MC), water vapour permeability (WVP) and thickness of S,
724 PVA and S:PVA blend films after 1 (t_0) and 5 (t_f) storage weeks. Mean values and
725 standard deviation.
726

	MC (%d.b.)		WVP (g.mm.kPa^{-1}h^{-1}m^{-2})		Thickness(mm)	
	t_0	t_f	t_0	t_f	t_0	t_f
S	6.9±0.2^{a1}	8.0±0.3^{a2}	5.3±0.3^{a1}	6.77 ±0.09^{a2}	0.078±0.008^{a1}	0.081±0.007^{a1}
PVA	5.03±0.06^{b1}	5.3±0.2^{b2}	2.2±0.2^{b1}	2.32±0.15^{b1}	0.13±0.03^{b1}	0.13±0.03^{b1}
S1:PVA2	6.6±0.8^{a1}	6.7±0.3^{c1}	3.5±0.3^{c1}	3.4±0.2^{c1}	0.11±0.03^{cd1}	0.104±0.014^{c1}
S1:PVA1	6.7±0.8^{a1}	7.3±0.4^{d1}	4.97±0.10^{d1}	4.7±0.2^{d1}	0.124±0.015^{bc1}	0.12±0.02^{d1}
S2:PVA1	6.9±0.5^{a1}	8.2±0.9^{a1}	5.7±0.4^{e1}	5.2±0.2^{e1}	0.11±0.03^{d1}	0.10±0.03^{c1}

727 ^{a,b,c,d,e} different letters in the same column indicate significant differences among formulations ($p<0.05$).

728 ^{1,2} different numbers in the same row indicate significant differences between storage times ($p<0.05$).

729

730 **Table 4.** The elastic modulus (EM), tensile strength at break (TS) and percentage of
731 elongation at break (ε, %) of S, PVA and S:PVA blend films after 1 (t_0) and 5 (t_f) storage
732 weeks. Mean values and standard deviation.
733

	EM (MPa)		TS (MPa)		E (%)	
	t_0	t_f	t_0	t_f	t_0	t_f
S	420 ± 40^{a1}	940 ± 90^{a2}	14.2 ± 1.3^{a1}	24 ± 3^{a2}	11 ± 2^{a1}	5.7 ± 1.9^{a2}
PVA	430 ± 90^{b1}	580 ± 80^{b2}	31 ± 5^{b1}	33 ± 3^{b1}	170 ± 50^{b1}	168 ± 19^{b1}
S1:PVA2	210 ± 60^{c1}	340 ± 50^{c2}	14 ± 2^{a1}	16 ± 3^{c1}	161 ± 16^{b1}	151 ± 30^{b1}
S1:PVA1	280 ± 60^{c1}	340 ± 70^{c2}	10.5 ± 1.9^{c1}	13 ± 3^{cd1}	80 ± 20^{c1}	93 ± 23^{1c}
S2:PVA1	272 ± 13^{c1}	420 ± 80^{d2}	9.5 ± 0.9^{c1}	10 ± 2^{d1}	58 ± 9^{c1}	33 ± 8^{a2}

734 ^{a,b,c,d} different letters in the same column indicate significant differences among formulations ($p<0.05$).
735 ^{1,2} different numbers in the same row indicate significant differences between storage times ($p<0.05$).
736

737 **Table 5.** The internal transmittance (Ti) at 450 nm and gloss values at 60º of S, PVA
738 and S:PVA blend films after 1 (t_0) and 5 (t_f) storage weeks. Mean values and standard
739 deviation.
740

	Ti (450 nm)		Gloss 60 º	
	t_0	t_f	t_0	t_f
S	84.38 ± 0.14^{a1}	83.9 ± 0.2^{a1}	27 ± 12^{a1}	18.9 ± 1.4^{a1}
PVA	85.9 ± 0.7^{b1}	85.1 ± 1.0^{b1}	153.9 ± 0.9^{b1}	145 ± 8^{b2}
S1:PVA2	85.27 ± 0.03^{b1}	85.4 ± 0.3^{b1}	18 ± 3^{c1}	20 ± 3^{a1}
S1:PVA1	85.5 ± 0.2^{b1}	85.09 ± 0.14^{b1}	14.0 ± 1.4^{c1}	17 ± 2^{a2}
S2:PVA1	85.53 ± 0.09^{b1}	85.77 ± 0.06^{b1}	13.2 ± 1.6^{c1}	12.9 ± 1.2^{a1}

741 ^{a,b,c} different letters in the same column indicate significant differences among formulations ($p<0.05$).
742 ^{1,2} different numbers in the same row indicate significant differences between storage times ($p<0.05$).
743

FIGURE CAPTIONS

Figure 1: FTIR spectra for S, PVA and S:PVA blend films.

Figure 2: FESEM micrographs of the surface and cross section of S and PVA films.

Figure 3: FESEM micrographs of the surface and cross section of S:PVA blend films.

Figure 4: a) TG and b) DTG curves of S, PVA and S:PVA blend films.

Figure 5: Typical strain-stress curves of S, PVA and S:PVA blend films at different storage times: a) one and b) five weeks.

Figure 6: UV-VIS spectra for S, PVA and S:PVA blend films.

753 **Figure 1.**

754

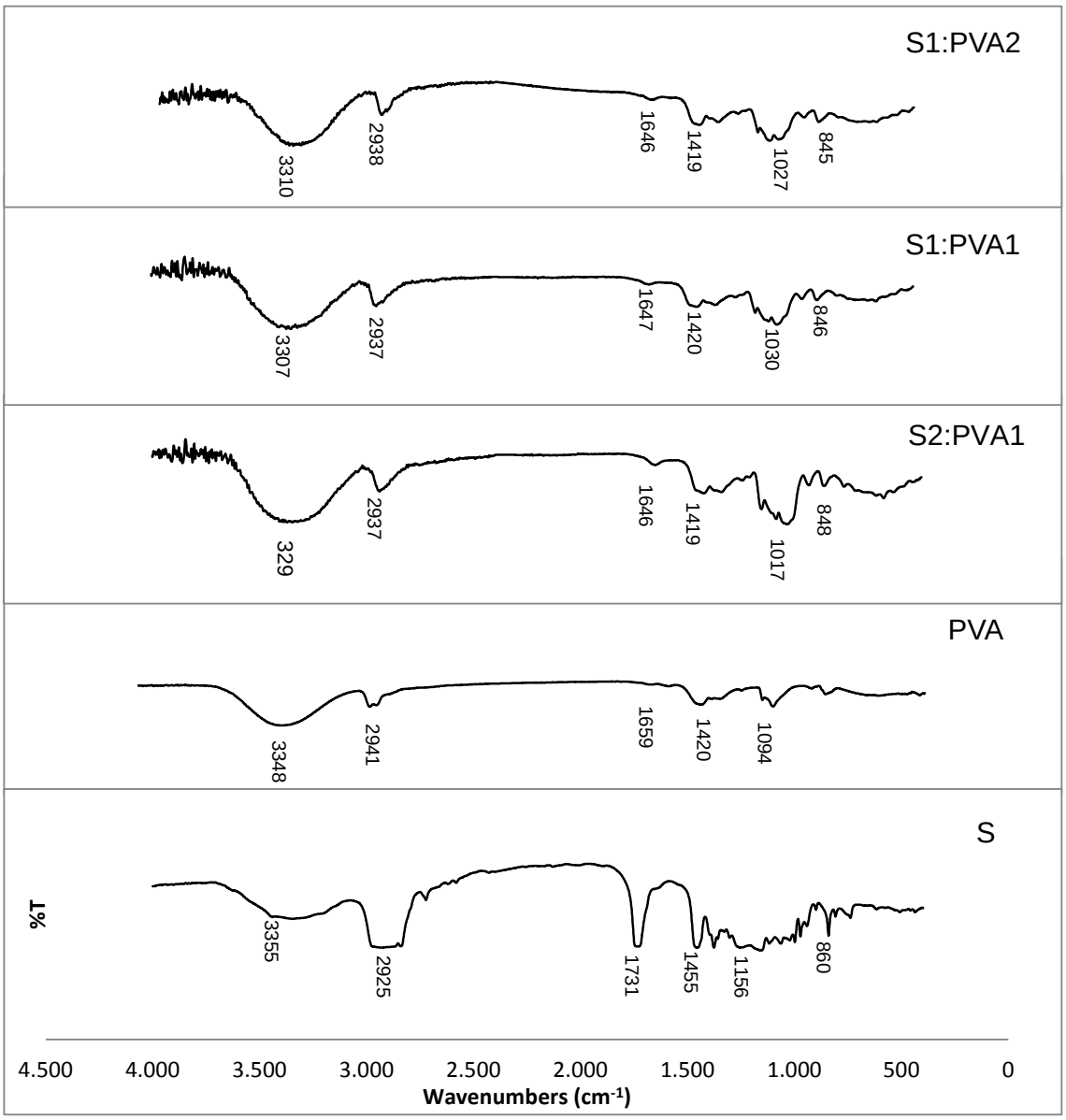

755

756

757

758

Figure 2.

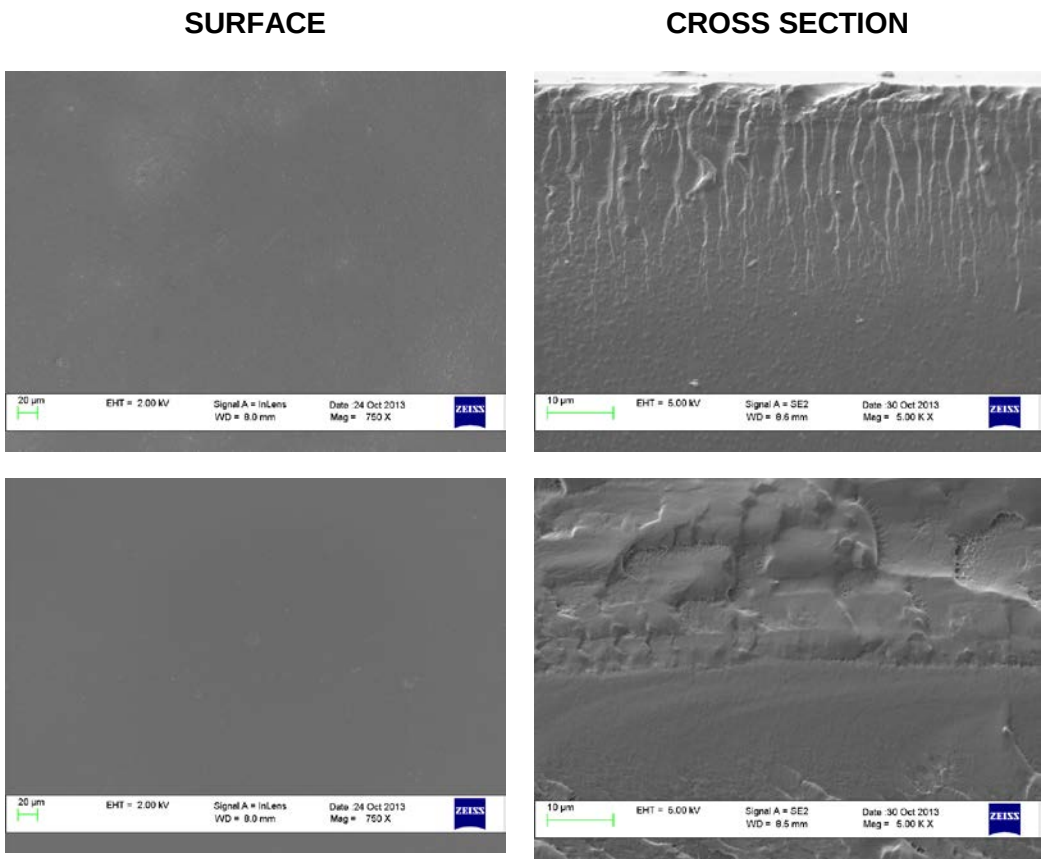
SURFACE
CROSS SECTION
S
PVA
20 µm
EHT = 2.00 kV
Signal A = InLens
WD = 9.0 mm
Date :24 Oct 2013
Mag = 750 X
ZEISS
10 µm
EHT = 5.00 kV
Signal A = SE2
WD = 8.6 mm
Date :30 Oct 2013
Mag = 5.00 K X
20 µm
EHT = 2.00 kV
Signal A = InLens
WD = 9.0 mm
Date :24 Oct 2013
Mag = 750 X
ZEISS
10 µm
EHT = 5.00 kV
Signal A = SE2
WD = 8.5 mm
Date :30 Oct 2013
Mag = 5.00 K X
ZEISS

764 **Figure 3.**

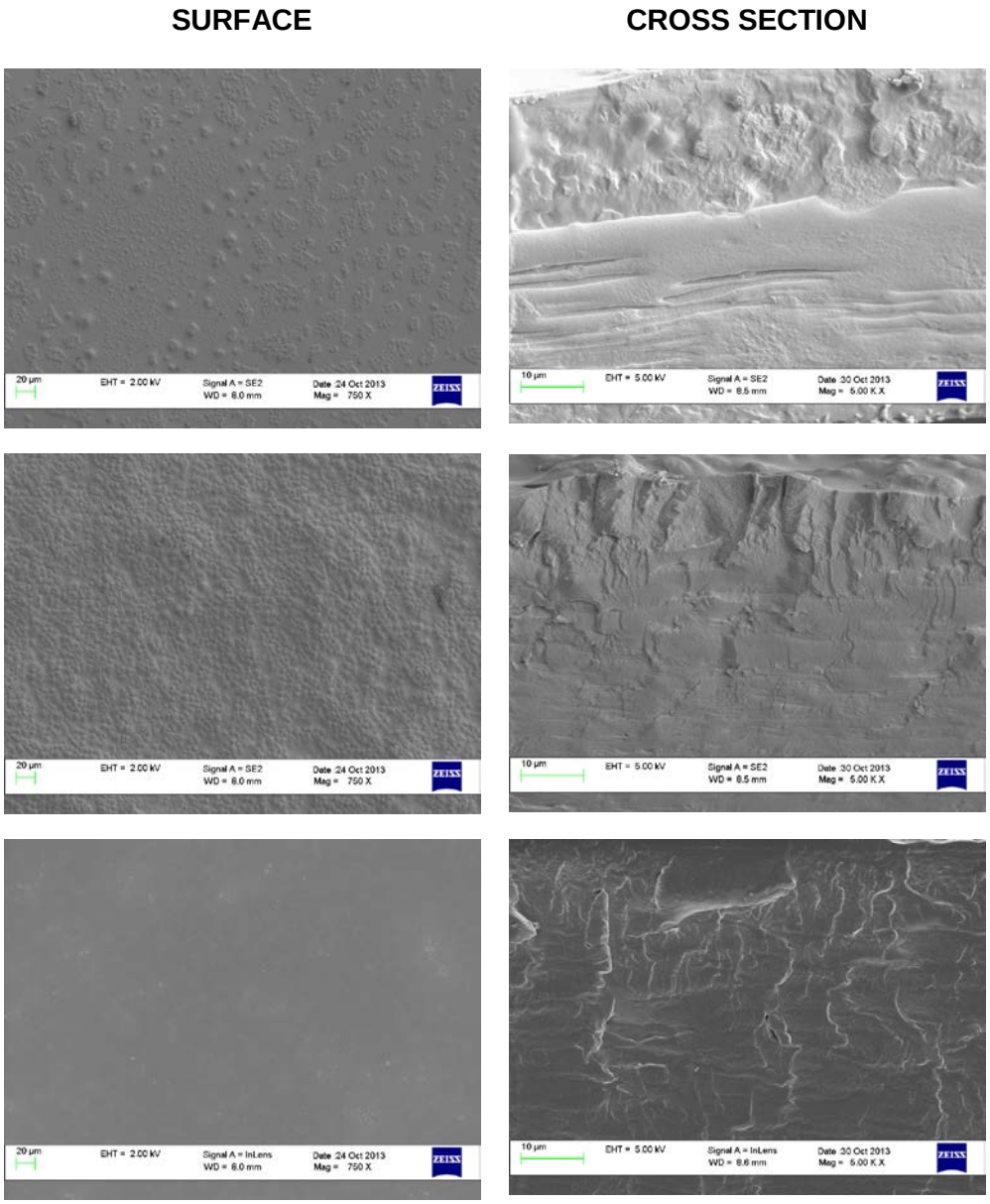

765

766 **Figure 4.**

767

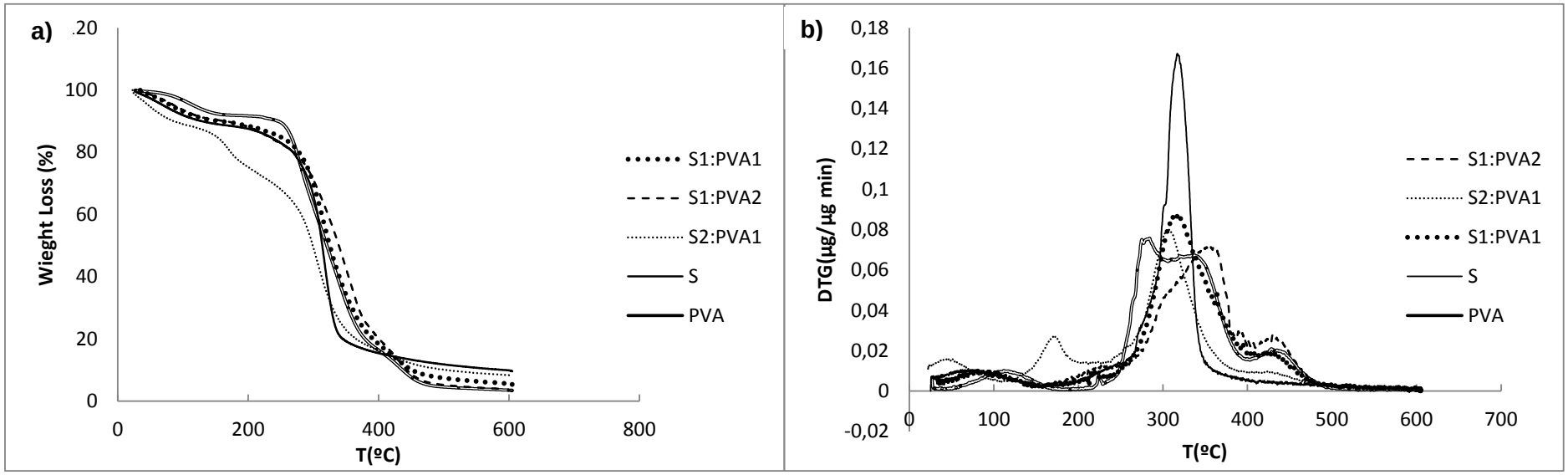

768

769

770

Figure 5.

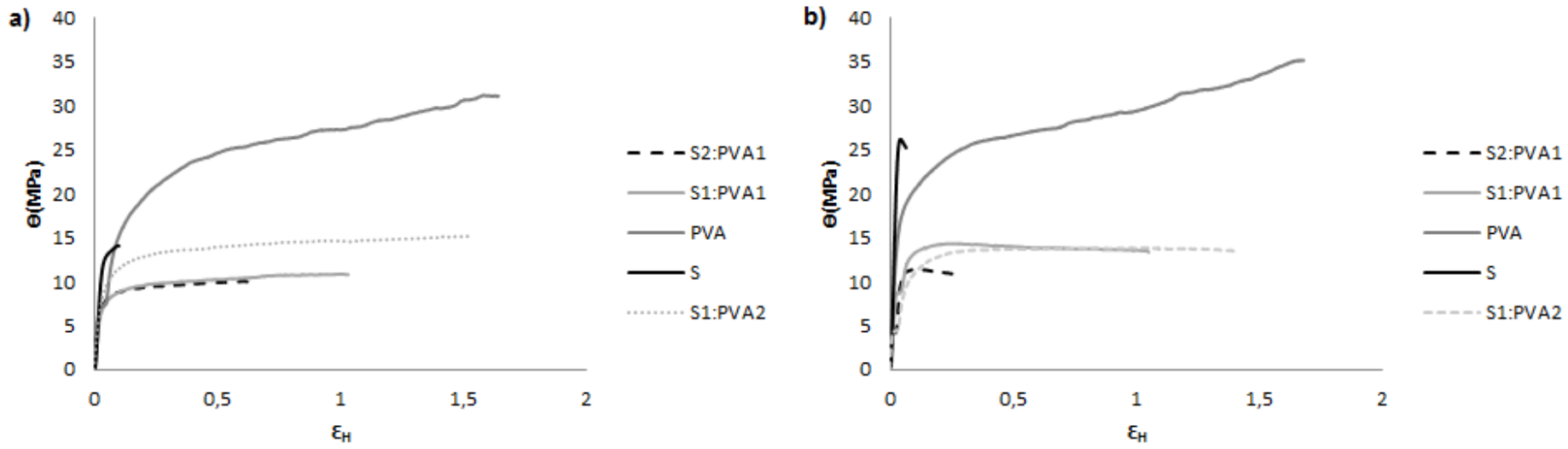

774 **Figure 6.**

775

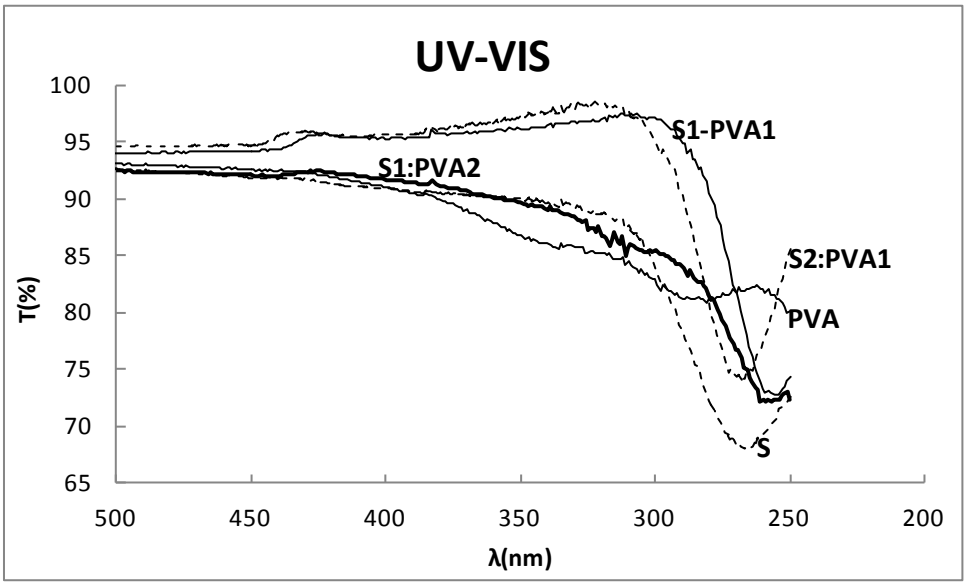

776

777

778